Finite-Temperature Relativistic Nuclear Field Theory: An Application to the Dipole Response

Elena Litvinova[1,2] and Herlik Wibowo[1]
[1]Department of Physics, Western Michigan University, Kalamazoo, Michigan 49008, USA
[2]National Superconducting Cyclotron Laboratory, Michigan State University, East Lansing, Michigan 48824, USA

(Received 1 May 2018; revised manuscript received 11 July 2018; published 22 August 2018)

Nuclear response theory beyond the one-loop approximation is formulated for the case of finite temperature. For this purpose, the time blocking approximation to the time-dependent part of the in-medium nucleon-nucleon interaction amplitude is adopted for the thermal (imaginary-time) Green's function formalism. We found that introducing a soft blocking, instead of a sharp blocking at zero temperature, brings the Bethe-Salpeter equation to a single-frequency variable equation also at finite temperatures. The method is implemented self-consistently in the framework of quantum hadrodynamics and designed to connect the high-energy scale of heavy mesons and the low-energy domain of nuclear medium polarization effects in a parameter-free way. In this framework, we investigate the temperature dependence of dipole spectra in the even-even nuclei ^{48}Ca and ^{100,120,132}Sn with a special focus on the giant dipole resonance's width problem and on the low-energy dipole strength distribution.

DOI: 10.1103/PhysRevLett.121.082501

Introduction.—The behavior of nuclear systems at finite temperature remains among the most difficult problems in nuclear theory. Nuclear temperature is a conventional concept for describing highly excited compound nuclei in long-lived intermediate states of such processes as neutron or proton capture, fusion, fission, and heavy ion collisions. An accurate description of the response of the compound nucleus to external probes and of its deexcitations is, therefore, of great importance for many applications, in particular, for nuclear data, nuclear technology, and modeling of astrophysical processes, including the evolution of stars and galaxies [1].

The dipole response, which dominates spectra of nuclear excitations, is commonly divided into the high-energy part, represented by the broad giant dipole resonance (GDR) associated with a high-frequency collective oscillation of protons and neutrons against each other, and the low-energy sector, the pygmy dipole resonance (PDR), which represents the oscillation of the neutron excess against the isospin-saturated core. As both of these structures have a very complex nature at the interface of coherent oscillations and pure particle-hole excitations, and their microscopic texture is linked to the astrophysical *r*-process nucleosynthesis, they continuously attract active interest from both experiment and theory [2].

An accurate theory for the response of compound nuclei, which is required most often for applications, is extremely challenging. The common practice is to confine the framework by the simplest one-loop approximation, such as thermal random phase approximation (TRPA) [3,4], thermal quasiparticle RPA (TQRPA) [3,5], or its version with exact pairing [6], and one step further is represented by the continuum TQRPA [7–9]. A few extensions of T(Q)RPA including damping mechanisms have been formulated, for instance, in Ref. [10] as the finite-temperature self-consistent RPA, Ref. [11] in terms of the collision integral with incoherent two-particle two-hole excitations, Ref. [12] as a coupling to collective surface vibrations in the framework of the nuclear field theory, and Refs. [13,14] as the finite-temperature second RPA by the equation of motion method. The numerical implementations of the approaches beyond T(Q)RPA are very scarce and mainly incomplete. For instance, Ref. [12] ignores coupling to noncollective modes and Ref. [11] does not include collective effects, which leads to the controversial results: the latter model concluded on a rapid increase of the GDR's width with temperature, while the former found the GDR nearly unchanged. The theories of thermal shape fluctuations [15,16] explain successfully the temperature dependence of the GDR's width found in experiments [17–20]; however, they do not provide microscopic details of the nuclear strength functions. The evolution of the low-energy strength with temperature, which is crucial for astrophysical modeling, is barely addressed in these calculations.

In this Letter, we present a new microscopic self-consistent approach to the nuclear response, which is free of the above mentioned limitations. We advance the approach developed previously in the zero-temperature framework of the relativistic nuclear field theory (RNFT) [21–23] to the finite-temperature case. The RNFT is based on the covariant energy density functional (CEDF) and extends the relativistic RPA (RRPA) beyond the one-loop approximation by taking into account the nonlinear medium polarization effects in a parameter-free way. This theory

performs very well when describing nuclear transitions from ground to excited states [2,24–34] and shows a similar potential for its finite-temperature generalization.

Formalism.—To determine microscopic characteristics of a compound nucleus, we apply the finite-temperature mean-field theory based on the variational principle of maximum entropy [35] with the CEDF of Ref. [36]. Here we consider nuclear systems without superfluid pairing, which include doubly magic nuclei and other systems at temperatures above the critical temperature. Thus, the eigenvalues of the nucleonic density matrix are the Fermi-Dirac occupation numbers

$$n_1(T) = n(\varepsilon_1, T) = \frac{1}{1 + e^{\varepsilon_1/T}}, \tag{1}$$

where the number index "1" runs over the complete set of the single-particle quantum numbers in the Dirac-Hartree basis, which includes the single-particle energies $\varepsilon_1 = \tilde{\varepsilon}_1 - \lambda$ measured from the chemical potential λ.

In order to compute the nuclear response to an external field of the particle-hole character, we have generalized the relativistic time blocking approximation of Ref. [22] to the case of finite temperature by adopting the time blocking technique to the Matsubara temperature Green's function formalism. The response function $\mathcal{R}_{14,23}(\omega, T)$ in the frequency (ω) domain, thus reads

$$\mathcal{R}_{14,23}(\omega, T) = \tilde{\mathcal{R}}_{14,23}(\omega, T) + \sum_{1'2'3'4'} \tilde{\mathcal{R}}_{12',21'}(\omega, T) \times \mathcal{W}_{1'4',2'3'}(\omega, T)\mathcal{R}_{3'4,4'3}(\omega, T), \tag{2}$$

where $\tilde{\mathcal{R}}(\omega, T)$ is the uncorrelated particle-hole propagator

$$\tilde{\mathcal{R}}_{14,23}(\omega, T) = \frac{n_{21}(T)\delta_{13}\delta_{24}}{\omega - \varepsilon_1 + \varepsilon_2}, \tag{3}$$

$n_{21}(T) = n_2(T) - n_1(T)$, and the interaction kernel transforms to the ω domain as

$$\mathcal{W}_{14,23}(\omega, T) = \tilde{V}_{14,23}(T) + \Phi_{14,23}(\omega, T) - \Phi_{14,23}(0, T). \tag{4}$$

The particle-vibration coupling (PVC) amplitude $\Phi(\omega, T)$ is given by

$$\Phi^{(ph)}_{14,23}(\omega, T) = \frac{1}{n_{43}(T)} \sum_{56\mu} \sum_{\eta_\mu = \pm 1} \eta_\mu \zeta^{\mu\eta_\mu}_{12,56} \zeta^{\mu\eta_\mu *}_{34,56} \times \frac{[N(\eta_\mu\Omega_\mu) + n_6(T)][n(\varepsilon_6 - \eta_\mu\Omega_\mu, T) - n_5(T)]}{\omega - \varepsilon_5 + \varepsilon_6 - \eta_\mu\Omega_\mu}, \tag{5}$$

where we denote the phonon vertex matrices $\zeta^{\mu\eta_\mu}$ as

$$\zeta^{\mu\eta_\mu}_{12,56} = \delta_{15}\gamma^{\eta_\mu}_{\mu;62} - \gamma^{\eta_\mu}_{\mu;15}\delta_{62}, \tag{6}$$

with the matrix elements of the particle-phonon coupling vertices $\gamma^{\eta_\mu}_{\mu;13} = \delta_{\eta_\mu,+1}\gamma_{\mu;13} + \delta_{\eta_\mu,-1}\gamma^*_{\mu;31}$ and the phonon frequencies as Ω_μ. The index μ numerates the phonon quantum numbers and, as in Ref. [22], the vertices $\gamma_{\mu;13}$ are extracted from the solution of Eq. (2) without the frequency-dependent interaction, which corresponds to the finite-temperature relativistic random phase approximation (FT-RRPA). The bosonic occupation factors $N(\Omega) = 1/(e^{\Omega/T} - 1)$ in Eq. (5) emerge as additional phonon characteristics. The hole-particle hp components of the amplitude $\Phi(\omega, T)$ are found analogously. At finite temperatures, we consider a pair of states $\{12\}$ as a ph pair if $n_{21}(T) > 0$ and as an hp pair if $n_{21}(T) < 0$, while pairs with $n_{21}(T) = 0$ are eliminated by Eq. (3). In Eq. (4), this amplitude is corrected by the subtraction of itself at zero frequency in order to avoid double counting of the particle-phonon coupling effects, which are implicitly included in the mean field, and provides a good convergence of the amplitude $\Phi(\omega, T)$ with respect to the phonon space [37,38]. The latter feature is widely utilized in applications as it allows a truncation of the phonon model space by the phonon energy ∼15–20 MeV in calculations for medium-heavy nuclei. At $T = 0$, $\Phi(\omega)$ is known to induce damping effects that lead to an additional fragmentation and broadening of the strength functions [22,23,39–41]. As it is shown below, at finite temperature, this amplitude plays a similar role.

Self-consistent calculations within the approach of Eqs. (2)–(6), named finite-temperature relativistic time blocking approximation (FT-RTBA), were performed in a wide range of temperatures for the dipole response of the three nuclei, ^{120,132}Sn and ^{48}Ca, for which we have obtained a very good description of data at $T = 0$ [23,24,34], and for an unstable ^{100}Sn nucleus with equal numbers of protons and neutrons ($N = Z$). For each temperature value, we solved first the self-consistent relativistic mean-field (RMF) problem with NL3 forces [42], which determined the meson and nucleon fields and the single-nucleon Dirac-Hartree basis. In this basis, the FT-RRPA problem with the same meson-exchange interaction was solved to obtain the vertices and frequencies of the phonon modes. The phonon space was truncated on angular momenta, frequencies, and reduced transition probabilities using the same criteria as in earlier calculations for $T = 0$. We included isoscalar phonon modes with natural parities and multipolarities $2 \le J_\mu \le 6$, frequencies $\Omega_\mu \le \Omega_c$ ($\Omega_c = 15$ MeV for ^{120,132}Sn and $\Omega_c = 20$ MeV for ^{48}Ca and ^{100}Sn), and the reduced transition probabilities exceeding 5% of the maximal one for each multipolarity. Keeping these criteria, we have included coupling to both collective and noncollective states while the total number of phonon modes grows by up to a factor of 10 at T ∼ 5–6 MeV, compared to $T = 0$. The selected phonon modes, together with the single-particle output of the thermal RMF, determine the particle-phonon coupling

amplitude $\Phi(\omega, T)$ and thus the response function of Eq. (2). Finally, the microscopic strength function $\tilde{S}(E, T)$ is defined as a response of a compound nucleus to an external field V^0 [3]: $\tilde{S}(E, T) = S(E, T)/(1 - e^{-E/T})$, where

$$S(E, T) = -\frac{1}{\pi} \lim_{\Delta \to +0} \mathrm{Im} \langle V^{0\dagger} \mathcal{R}(E + i\Delta, T) V^0 \rangle, \quad (7)$$

with V^0 being a dipole operator and with a finite value of the imaginary part of the energy variable Δ, which accounts for missing effects of higher-order configurations and the continuum [23].

Results.—The results for the dipole strength distributions $S(E, T)$ in a medium-light ^{48}Ca nucleus and in medium-heavy ^{100,120,132}Sn nuclei at various temperatures are displayed in Figs. 1 and 2, where we compare the evolution of the strength within FT-RRPA and FT-RTBA. In ^{48}Ca, we observe the two major effects with the temperature increase: a continuous broadening and a quenching of the GDR and an enhancement of the low-energy strength associated with the PDR. This evolution is accompanied by a slow movement of the entire distribution towards the lower energy. At $T \approx 5$–6 MeV, the low-energy part begins to dominate for all multipoles, which in turn reinforces the damping of the GDR. These temperatures are consistent with the limit of existence of the GDR established in earlier works [43]. The obtained evolution of the dipole strength with the temperature increase is caused by (i) a slow change of the self-consistent mean field and of the single-particle orbits of the compound nucleus, (ii) the increasing diffuseness of the Fermi surface, which enhances the amount of the low-energy particle-hole configurations and reinforces the Landau damping, and (iii) a reduction of the leading contribution to the particle-phonon coupling amplitude (5) associated with $\eta_\mu = 1$, which is the only contribution at $T = 0$, and an increasing role of the new terms with $\eta_\mu = -1$.

The trends are similar in the medium-heavy tin nuclei. ^{120}Sn is superfluid below the critical temperature $T_c \approx 0.66$ MeV in our framework and ^{100,132}Sn have closed shells in both proton and neutron subsystems. Thus, the GDR's width in ^{120}Sn decreases in the temperature interval $0 \le T \le T_c$ and begins to increase at $T > T_c$, while the GDR's widths in ^{100,132}Sn grow in the entire temperature range. Comparing right and left panels of Figs. 1 and 2, one can notice that the fragmentation effect of the PVC mechanism is relatively weak for the excited states emerging with the temperature increase at low energy. These states are absent at $T = 0$ and formed solely by the transitions within thermally unblocked pairs. It turns out that for such pairs of states the matrix elements of the PVC amplitude $\Phi(\omega)$ are strongly suppressed by the factor in the numerator of Eq. (5), $n(\varepsilon_6 - \eta_\mu \Omega_\mu, T) - n_5(T)$. Thus, the lack of fragmentation of the thermally unblocked states is probably due to some limitations of our approach: the PVC amplitude $\Phi(\omega)$ includes only the so-called resonant part and does not include the ground state correlations (GSC) induced by the PVC. The structure of these GSC-PVC terms at $T = 0$ [44] points out that they may enforce the fragmentation effect on the thermally unblocked transitions. The inclusion of these effects for $T > 0$ will be considered elsewhere.

The temperature dependence of the GDR's width $\Gamma(T)$ obtained in FT-RTBA is shown in Fig. 3(a) for ^{132}Sn and

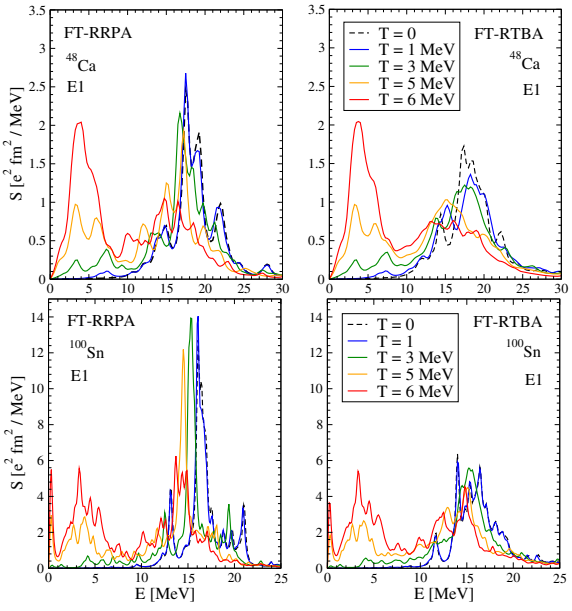

FIG. 1. Electric dipole strength distribution in ^{48}Ca and ^{100}Sn calculated within FT-RRPA (left) and FT-RTBA (right) at various temperatures. The values of the imaginary part of the energy variable $\Delta = 500$ and 200 keV were adopted for ^{48}Ca and ^{100}Sn, respectively.

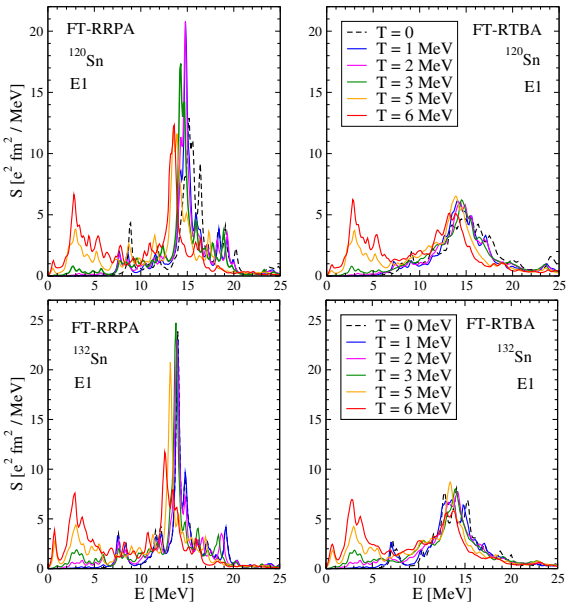

FIG. 2. Same as in Fig. 1 but for ^{120,132}Sn with $\Delta = 200$ keV.

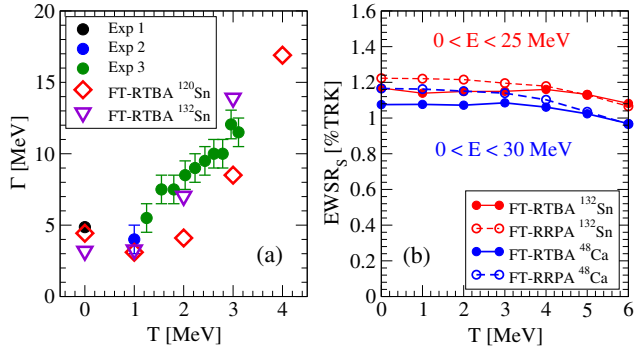

FIG. 3. (a) Width of the giant dipole resonance in ^{120,132}Sn as a function of temperature. The experimental values from Refs. [20,45,46] are shown for ^{120}Sn. (b) The EWSR for ^{48}Ca and ^{132}Sn with respect to the TRK sum rule.

^{120}Sn together with experimental data available for ^{120}Sn. The theoretical widths at $T = 0$ are taken from our previous calculations [22,23]. The nucleus ^{120}Sn is superfluid below $T \sim 0.66$ MeV and the ^{132}Sn one is nonsuperfluid. Because of the phase transition in ^{120}Sn at $T \approx 0.66$ MeV, $\Gamma(T)$ has a smaller value at $T = 1$ MeV than at $T = 0$ as disappearance of the superfluid pairing reduces the width. Thermal effects are not yet seen at $T = 1$ MeV because of specific shell structure of ^{120}Sn. When the temperature starts to increase, the protons that form the closed shell have the next available orbitals only in the next major shell, and $T = 1$ MeV temperature is not sufficient to promote the protons over the shell gap with a noticeable occupancy. In the neutron subsystem, the lowest available orbit is the intruder $1h_{11/2}$ state, where particles get promoted relatively easily, but after this orbit there is another shell gap. As a consequence, at $T = 1$ MeV there is still no room for a noticeable thermal unblocking. Thus, our result can explain the unexpectedly small GDR's width at $T = 1$ MeV reported in Ref. [45], in contrast to the thermal shape fluctuation calculations.

In ^{132}Sn, we observe a relatively fast increase of $\Gamma(T)$ after $T = 1$ MeV and no increase below this temperature because of the presence of the shell gaps in both proton and neutron subsystems. After $T = 1$ MeV in ^{132}Sn and $T = 2$ MeV in ^{120}Sn, we obtain a fast increase of $\Gamma(T)$ because of (i) the formation of the low-energy shoulder and (ii) a slow increase of the fragmentation of the high-energy peak, which becomes faster at high temperatures when the low-energy phonons develop the new sort of collectivity. As ^{132}Sn is more neutron-rich than ^{120}Sn, the respective strength in the low-energy shoulder of ^{132}Sn is larger, which leads to a larger overall width in ^{132}Sn at temperatures above 1 MeV. Note that $\Gamma(T)$ values for $T > 3$ MeV in ^{132}Sn and at $T > 4$ MeV in ^{120}Sn are not presented because the standard procedure based on the Lorentzian fit of the microscopic strength distribution fails in recognizing the distribution as a single-peak structure.

For ^{120}Sn, we find a good agreement with data for $T = 0$, $T = 1$ MeV and a reasonable agreement for $T = 3$ MeV. The discrepancy at $T = 2$ MeV can be due to the fact that, in the experimental studies in this temperature range, compound nuclei acquire nonzero angular momenta up to $60\hbar$. This, in turn, increases the total width of the GDR [47]. We do not have such effects included in the presented approach, but they can be considered in future work. It is also established experimentally that, at temperatures around 3 MeV, the angular momentum dependence of the GDR's width in tin nuclei is saturated [43], which is consistent with our finding that at $T = 3$ MeV our calculated $\Gamma(T)$ in ^{120}Sn is getting much closer to the data.

Figure 3(b) illustrates the evolution of the dipole energy-weighted some rule (EWSR), which is given in percent with respect to the Thomas-Reiche-Kuhn (TRK) sum rule, in ^{48}Ca and ^{132}Sn. As shown in Ref. [48], the EWSR at $T > 0$ can be calculated in full analogy with the case of $T = 0$. Since the meson-exchange interaction is velocity dependent, already in RRPA and its superfluid version at $T = 0$, we observe up to 40% enhancement of the TRK sum rule within the experimentally studied energy regions [22,23], in agreement with data. In the resonant time blocking approximation without the GSC-PVC, the EWSR should have exactly the same value as in RPA; however, the subtraction procedure causes a little violation of it [37,49]. In the RTBA vs RRPA at $T = 0$, we usually find a few percent less in finite-energy intervals below 25–30 MeV, but this difference decreases if we take larger intervals, since in RTBA the strength distributions are more spread and have heavier high-energy tails. A similar situation takes place at $T > 0$. Figure 3(b) shows a slow decrease of the EWSR with temperature because the entire resonance moves down in energy while FT-RRPA and FT-RTBA values practically meet at $T = 6$ MeV when their high-energy tails become less important.

Figure 4 displays the temperature evolution of transition densities in the neutron and proton subsystems of the

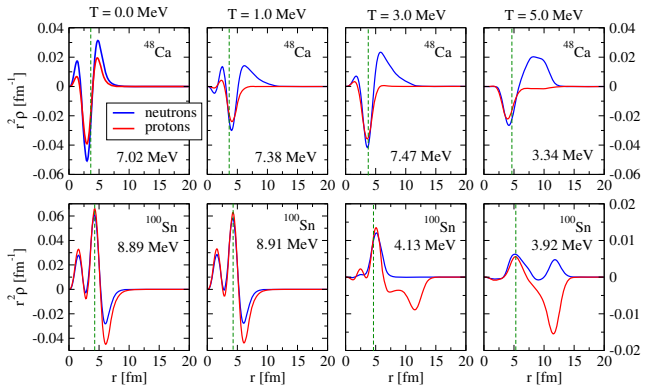

FIG. 4. Temperature evolution of the proton and neutron transition densities for the most prominent peaks below 10 MeV in ^{48}Ca and ^{100}Sn within FT-RTBA. The dashed vertical lines indicate the rms nuclear radius.

neutron-rich ^{48}Ca in comparison to those of the $N = Z$ neutron-deficient ^{100}Sn, for their strongest peaks below 10 MeV. This energy region is typically associated with the PDR. One can see that at all temperatures ^{48}Ca shows a usual pattern of the in-phase oscillation of protons and neutrons inside the nucleus, while the neutron oscillation dominates in the outside area. The radial transition densities become more extended with the temperature growth, but qualitatively, their behavior remains similar. An analogous situation occurs in ^{100}Sn, but with the proton dominance outside. The entire PDR slowly moves toward lower energies with the temperature growth in both nuclei. Large spatial extensions of the radial transition density distributions for the leading low-energy peaks at high temperatures may point to approaching the limits of existence of the considered nuclear systems.

Summary.—We present an advanced microscopic self-consistent many-body approach to the finite-temperature nuclear response, which includes spreading effects, in addition to Landau damping. In this framework, we investigated the evolution of the dipole strength distribution in medium-mass nuclei in a wide range of temperatures. The obtained results are consistent with the existing experimental data on the GDR's width and with the Landau theory [50], explain the critical phenomenon of the disappearance of the GDR at high temperatures, and predict the evolution of the low-energy dipole strength with temperature, taking into account spreading effects.

The analytical method presented in this Letter is quite general and can be widely applied to investigate the response of strongly correlated systems at finite temperature. The presented numerical implementation of the developed approach opens a way to accurate systematic studies of excitations and deexcitations of compound nuclei in a wide energy range. Both giant resonances and soft modes of various multipolarities in medium-heavy nuclei are of primary interest in this context because of their direct implications for *r*-process nucleosynthesis. Such systematic studies will be addressed by future efforts.

The authors greatly appreciate discussions with P. Schuck and D. Halderson. This work is partly supported by US-NSF Grant No. PHY-1404343 and by NSF Career Grant No. PHY-1654379.

[1] M. Mumpower, R. Surman, G. McLaughlin, and A. Aprahamian, Prog. Part. Nucl. Phys. **86**, 86 (2016).
[2] D. Savran, T. Aumann, and A. Zilges, Prog. Part. Nucl. Phys. **70**, 210 (2013).
[3] P. Ring, L. M. Robledo, J. L. Egido, and M. Faber, Nucl. Phys. **A419**, 261 (1984).
[4] Y. F. Niu, N. Paar, D. Vretenar, and J. Meng, Phys. Lett. **681B**, 315 (2009).
[5] E. Yüksel, G. Colò, E. Khan, Y. F. Niu, and K. Bozkurt, Phys. Rev. C **96**, 024303 (2017).
[6] N. Q. Hung, N. D. Dang, and L. T. Q. Huong, Phys. Rev. Lett. **118**, 022502 (2017).
[7] E. Litvinova, S. Kamerdzhiev, and V. Tselyaev, Phys. At. Nucl. **66**, 558 (2003).
[8] E. Khan, N. Van Giai, and M. Grasso, Nucl. Phys. **A731**, 311 (2004).
[9] E. Litvinova and N. Belov, Phys. Rev. C **88**, 031302 (2013).
[10] J. Dukelsky, G. Röpke, and P. Schuck, Nucl. Phys. **A628**, 17 (1998).
[11] D. Lacroix, P. Chomaz, and S. Ayik, Phys. Rev. C **58**, 2154 (1998).
[12] P. Bortignon, R. Broglia, G. Bertsch, and J. Pacheco, Nucl. Phys. **A460**, 149 (1986).
[13] S. Adachi and P. Schuck, Nucl. Phys. **A496**, 485 (1989).
[14] C. Yannouleas and S. Jang, Nucl. Phys. **A455**, 40 (1986).
[15] D. Kusnezov, Y. Alhassid, and K. A. Snover, Phys. Rev. Lett. **81**, 542 (1998).
[16] W. E. Ormand, P. F. Bortignon, and R. A. Broglia, Phys. Rev. Lett. **77**, 607 (1996).
[17] J. J. Gaardhøje, C. Ellegaard, B. Herskind, and S. G. Steadman, Phys. Rev. Lett. **53**, 148 (1984).
[18] J. J. Gaardhøje, C. Ellegaard, B. Herskind, R. M. Diamond, M. A. Deleplanque, G. Dines, A. O. Macchiavelli, and F. S. Stephens, Phys. Rev. Lett. **56**, 1783 (1986).
[19] A. Bracco, J. Gaardhøje, A. Bruce, J. Garrett, B. Herskind, M. Pignanelli, D. Barneoud, H. Nifenecker, J. Pinston, C. Ristori *et al.*, Phys. Rev. Lett. **62**, 2080 (1989).
[20] E. Ramakrishnan, T. Baumann, A. Azhari, R. Kryger, R. Pfaff, M. Thoennessen, S. Yokoyama, J. Beene, M. Halbert, P. Mueller *et al.*, Phys. Rev. Lett. **76**, 2025 (1996).
[21] E. Litvinova and P. Ring, Phys. Rev. C **73**, 044328 (2006).
[22] E. Litvinova, P. Ring, and V. Tselyaev, Phys. Rev. C **75**, 064308 (2007).
[23] E. Litvinova, P. Ring, and V. Tselyaev, Phys. Rev. C **78**, 014312 (2008).
[24] E. Litvinova, P. Ring, V. Tselyaev, and K. Langanke, Phys. Rev. C **79**, 054312 (2009).
[25] E. Litvinova, H. Loens, K. Langanke, G. Martinez-Pinedo, T. Rauscher, P. Ring, F.-K. Thielemann, and V. Tselyaev, Nucl. Phys. **A823**, 26 (2009).
[26] E. Litvinova, P. Ring, and V. Tselyaev, Phys. Rev. Lett. **105**, 022502 (2010).
[27] J. Endres, E. Litvinova, D. Savran, P. A. Butler, M. N. Harakeh, S. Harissopulos, R.-D. Herzberg, R. Krücken, A. Lagoyannis, N. Pietralla, V. Y. Ponomarev, L. Popescu, P. Ring, M. Scheck, K. Sonnabend, V. I. Stoica, H. J. Wörtche, and A. Zilges, Phys. Rev. Lett. **105**, 212503 (2010).
[28] A. Tamii *et al.*, Phys. Rev. Lett. **107**, 062502 (2011).
[29] R. Massarczyk, R. Schwengner, F. Dönau, E. Litvinova, G. Rusev, R. Beyer, R. Hannaske, A. Junghans, M. Kempe, J. H. Kelley *et al.*, Phys. Rev. C **86**, 014319 (2012).
[30] E. Litvinova, P. Ring, and V. Tselyaev, Phys. Rev. C **88**, 044320 (2013).
[31] E. G. Lanza, A. Vitturi, E. Litvinova, and D. Savran, Phys. Rev. C **89**, 041601 (2014).
[32] I. Poltoratska, R. W. Fearick, A. M. Krumbholz, E. Litvinova, H. Matsubara, P. von Neumann-Cosel, V. Y. Ponomarev, A. Richter, and A. Tamii, Phys. Rev. C **89**, 054322 (2014).

[33] B. Özel-Tashenov, J. Enders, H. Lenske, A. M. Krumbholz, E. Litvinova, P. von Neumann-Cosel, I. Poltoratska, A. Richter, G. Rusev, D. Savran, and N. Tsoneva, Phys. Rev. C **90**, 024304 (2014).
[34] I. A. Egorova and E. Litvinova, Phys. Rev. C **94**, 034322 (2016).
[35] H. M. Sommermann, Ann. Phys. (N.Y.) **151**, 163 (1983).
[36] D. Vretenar, A. V. Afanasjev, G. A. Lalazissis, and P. Ring, Phys. Rep. **409**, 101 (2005).
[37] V. I. Tselyaev, Phys. Rev. C **75**, 024306 (2007).
[38] V. I. Tselyaev, Phys. Rev. C **88**, 054301 (2013).
[39] T. Marketin, E. Litvinova, D. Vretenar, and P. Ring, Phys. Lett. **706B**, 477 (2012).
[40] E. Litvinova, B. Brown, D.-L. Fang, T. Marketin, and R. Zegers, Phys. Lett. **730B**, 307 (2014).
[41] C. Robin and E. Litvinova, Eur. Phys. J. A **52**, 205 (2016).
[42] G. A. Lalazissis, J. König, and P. Ring, Phys. Rev. C **55**, 540 (1997).
[43] D. Santonocito and Y. Blumenfeld, in *Dynamics and Thermodynamics with Nuclear Degrees of Freedom* (Springer, New York, 2006) p. 183.
[44] S. P. Kamerdzhiev, G. Y. Tertychny, and V. I. Tselyaev, Phys. Part. Nucl. **28**, 134 (1997).
[45] P. Heckman, D. Bazin, J. Beene, Y. Blumenfeld, M. Chromik, M. Halbert, J. Liang, E. Mohrmann, T. Nakamura, A. Navin *et al.*, Phys. Lett. **555B**, 43 (2003).
[46] S. Fultz, B. Berman, J. Caldwell, R. Bramblett, and M. Kelly, Phys. Rev. **186**, 1255 (1969).
[47] M. Mattiuzzi, A. Bracco, F. Camera, W. E. Ormand, J. J. Gaardhøje, A. Maj, B. Million, M. Pignanelli, and T. Tveter, Nucl. Phys. **A612**, 262 (1997).
[48] M. Barranco, A. Polls, and J. Martorell, Nucl. Phys. **A444**, 445 (1985).
[49] E. V. Litvinova and V. I. Tselyaev, Phys. Rev. C **75**, 054318 (2007).
[50] L. Landau, JETP **5**, 101 (1957).